

# Supplement Data

## In situ study on the structure evolution of ionic gel flexible sensors

Shujun Yan <sup>1</sup>, Jun Tang <sup>2,3,\*</sup>, Zhengwei Jin <sup>1</sup>, Nie Zhao <sup>2,3</sup>, Angui Zhang <sup>1</sup>, Shaowei Sun <sup>4,\*</sup>

<sup>1</sup> National Energy Group Ningxia Coal Industry Co., Ltd., Ningxia 750001, China;

<sup>2</sup> School of Materials Science and Engineering, Xiangtan University, Xiangtan 411105, China;

<sup>3</sup> Hunan Bangzer Technology Co., Ltd, Xiangtan 411100, China;

<sup>4</sup> School of Energy and Power Engineering, Xi'an Jiaotong University, Xi'an 710049, China;

\* Corresponding author: JunTang123@outlook.com and shaowei\_sun98@163.com.

### S1. Materials

The material used in this study is an amphiphilic poly (ethylene oxide)–poly (propylene oxide)-based (F127) triblock copolymers obtained from Sigma-Aldrich and used as received. The sample has a reported MW = 12600, PEO<sub>106</sub>-PPO<sub>70</sub>-PEO<sub>106</sub>. This material is very similar to a polymer studied extensively by Lopez-Barron and co-workers, who reported an order–disorder transition (ODT) at approximately 24 °C. The microphase-separated structure was found to depend on the thermal history of the sample. However, the viscoelasticity of these solutions is highly enhanced without detriment to their ionic conductivity. In the case of the solutions with compositions near the sol–gel transition, crosslinking produces soft elastomers with an outstanding tensile response, whose structure and shear modulus respond reversibly to temperature changes. Hexagonal close-packed structures (HCP) are formed when the sample is stretched.

Synthesis of Pluronic F127 Diacrylate (FDA). FDA was synthesized following the procedure reported by Cellesi et al[1]. In short, 50 g of Pluronic F127 was dissolved in toluene by slow stirring at room temperature under a nitrogen atmosphere. The mixture was cooled down to 0 °C using an ice bath. Acrylation of the hydroxyl groups of F127 was achieved by sequential addition of 2.4 mL of triethylamine, 40 mL of dichloromethane, and 1 mL of acryloyl chloride dissolved in 40 mL of dichloromethane, followed by stirring for 12 h under nitrogen gas. The precipitated triethylammonium chloride was filtered away, and the solvent evaporated using a rotary evaporator until a viscous oil was obtained. The latter was dissolved in dichloromethane, washed with DI water, and dried over sodium sulfate. The product FDA was precipitated into excess chilled diethyl ether. The white precipitate was dried under a vacuum for 1 day.

### S2. Correlation function.

Two primary types of analysis are performed on X-ray scattering images. Intensity as a function of scattering vector is extracted in 10° wide sectors of the image parallel (azimuthal angle 175°-195°) and perpendicular (85°-95°) to the flow direction using the program Fit2D. I(q) plots reveal the microphase-separated morphology as well as characteristic domain spacing (d-spacing). Flow-induced changes in primary peak location (q\*) both parallel and perpendicular to the flow direction are determined from polynomial fits of data near the primary diffraction peak, allowing extraction of corresponding d-

spacing values according to  $d = 2\pi/q^*$ . Intensity is extracted as a function of azimuthal angle  $\varphi$  over a  $q$  range that spans the primary diffraction peak, focusing on the top half of the image ( $\varphi = 0-180^\circ$ ) to avoid the shadow from the beam stop holder in the bottom of the image. Underflow, the diffraction peak location is dependent on an azimuthal angle. To ensure consistency in the extraction of azimuthal scans under these conditions, the azimuthal scan  $I(\varphi)$  is computed according to (1)[2].

$$I(\varphi) = \int_{1-\delta}^{1+\delta} I(q_r, \varphi) dq_r \quad (1)$$

where  $q_r = q/q^*(\varphi)$ . Thus, the range of  $q$  used in computing  $I(\varphi)$  (depicted as circular in Figure 2a) is made to conform to the elliptical distortion of the primary diffraction peak in the 2D scattering images. In our analyses,  $\delta$  is set equal to 0.35. The azimuthal distribution of intensity is related to the orientation distribution of the “six-point” features. Given the nearly random initial condition and uniaxial symmetry of the applied flow, the orientation distribution itself should exhibit uniaxial symmetry, such that the degree of microdomain orientation may be quantified in terms of Hermann’s orientation parameter,  $\langle P_2 \rangle$ . This is defined as the average of  $P_2(\cos \varphi) = 3/2(\cos 2\varphi - 1)$ , weighted by the uniaxial orientation probability distribution function  $f(\varphi)$ . Since cylindrical microdomains diffract perpendicularly to their axes,  $I(\varphi)$  is not itself equal to  $f(\varphi)$  but is rather related to  $f(\varphi)$  via an Abel transformation[3]. Nevertheless, the orientation parameter may be computed by first calculating an average of  $P_2$  weighted by  $I(\varphi)$ , and then normalizing by the value ( $= -1/2$ ) that would be realized for a perfectly oriented sample with intensity concentrated at  $\varphi = \pi/2$ . The resulting expression is (2).

$$\langle P_2 \rangle = - \frac{2 \int_0^\pi P_2(\cos \varphi) \sin \varphi I(\varphi) d\varphi}{\int_0^\pi \sin \varphi I(\varphi) d\varphi} \quad (2)$$

Defined in this way,  $\langle P_2 \rangle = 0$  for a random orientation and approaches a value of 1 for the perfect orientation of microdomains along the stretching direction. In this work, we measure the relaxation of several physical quantities: mechanical stress, X-ray orientation parameter, and d-spacing. To quantify and compactly represent the rates of these relaxation processes, we fit data using a multimode decaying exponential function: (3)

$$g(t) = \sum_i a_i e^{-t/\lambda_i} + b \quad (3)$$

where  $g(t)$  represents relaxation data from a particular experiment and variable. This function includes a constant baseline term ( $b$ ) since many of the quantities being studied here do not relax to a zero value. From such fits, we calculated an average relaxation time according to (4).

$$\lambda_{avg} = \frac{\sum a_i \lambda_i}{\sum a_i} \quad (4)$$

### S3 Electrical properties of EAN/F127DA ionic gel

In order to verify whether the EAN/F127DA ionic gel is conductive, it is connected to the LED lamp and battery through the EAN/F127DA ionic gel, and the bulb is lit, which

proves that the EAN/F127DA ionic gel is a good ionic conductor, as shown in Figure 1(a). When the EAN/F127DA ionic gel is stretched, the bulb lights up, which is different from the characteristics of other materials, indicating that the resistance value of the EAN/F127DA ionic gel does not increase but decreases during the stretching process, which is still the result of repeated several times, and the mechanism needs to be further explored. The ion conductivity of IG<sub>75%</sub> ion gel measured by electrical impedance spectroscopy at 25 °C is 15 mS/cm, half of that of pure EAN (28 mS/cm).

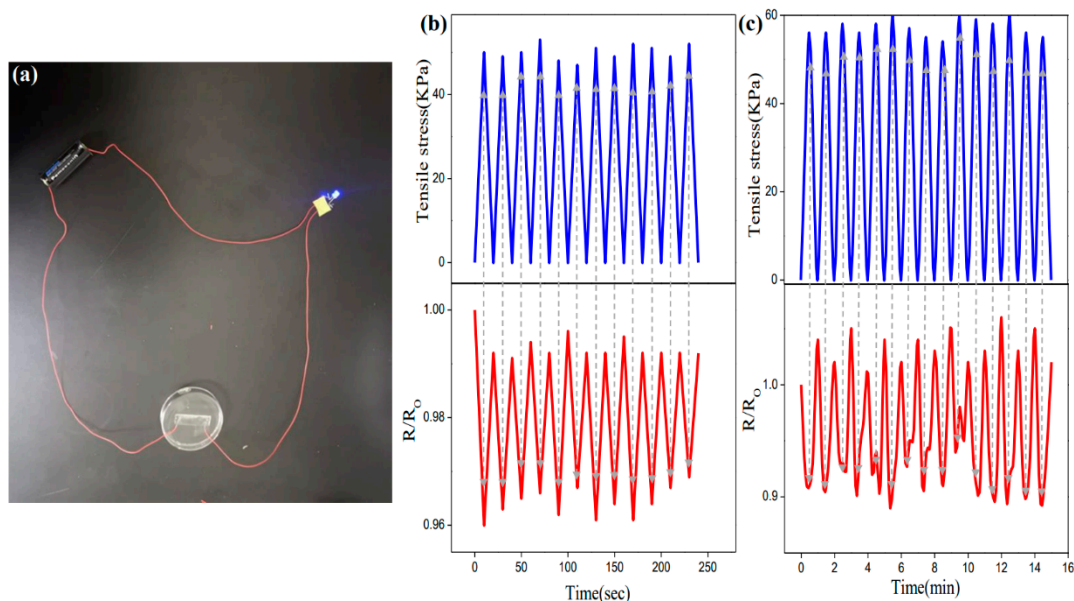


Figure S1. IG<sub>75%</sub> ion gel: (a) connect the LED; (b) Stress normalized resistance change curve of repeated stretching recovery cycle for 240 seconds; (c) Stress normalized resistance change curve after repeated stretching recovery cycle for 15 minutes.

The stability of electromechanical response is the key to studying stretchable electronic devices. Use KW tensile tester and KEITHLEY 6517B to conduct tensile and electrical measurement at the same time. The end of EAN/F127DA ion gel sample is bonded to the clamp of the tensile tester and then connected to the copper wire of KEITHLEY-6517B. The resistance  $R/R_0$  (where  $R_0$  is the ion resistance before stretching) of the normalized EAN/F127DA ion gel measured with an ohmmeter is plotted in Figure 1 (b) during the repeated stretching recovery cycle for 240 s. Obviously, the response and deformation of EAN/F127DA ionic gel resistance go on at the same time, and become inversely proportional to the strain. For larger strains (as shown in Figure 1 (c)), the corresponding resistance values are also lower. The resistance of EAN/F127DA ionic gel decreases with the increase of strain, which is counter intuitive, because the conductivity  $\sigma$  for materials with constant volume  $V$ , the ion resistance is

$$R = \frac{L \cdot \sigma}{A} \quad (5)$$

Where  $L$  is the length of the sample and  $A$  is its cross-sectional area. Please note that,  $\sigma$  It is the conductivity (determined by the material itself). Unless there is a change in the microstructure or chemical composition of the material  $\sigma$  There will be no change. Stretching ionic gel involves increasing  $L$  and decreasing  $A$ , which will lead to an increase in ionic resistance. This situation was observed in the resistance measurement of EAN/F127DA ionic gel, indicating that the inherent conductivity of ionic gel materials changed due to the rearrangement of microstructure during the tensile process. During the reply process, the ion resistance almost increased to the original value ( $R_0$ ), indicating that the microstructure has largely recovered its original configuration as shown in Figure 1 (b).

#### ***S4 Response stability of EAN/F127DA ionic gel***

In order to test the response stability of EAN/F127DA ionic gel, IG<sub>75%</sub> ionic gel was stretched to 50% strain for 1000 cycles, and its resistance value was measured continuously during the cycle. It can be observed that  $R/R_0$  oscillates repeatedly between 0.85 and 1.06, as shown in Figure 2 (a). In order to better present the amplification of Figure 2 (b) in the range of 5000 s to 5500 s. The results showed that the ionic gel responded in time during the stretch recovery cycle, without signal weakening. This is in line with the original design intention, indicating that EAN/F127DA ionic gel can be used for practical applications.

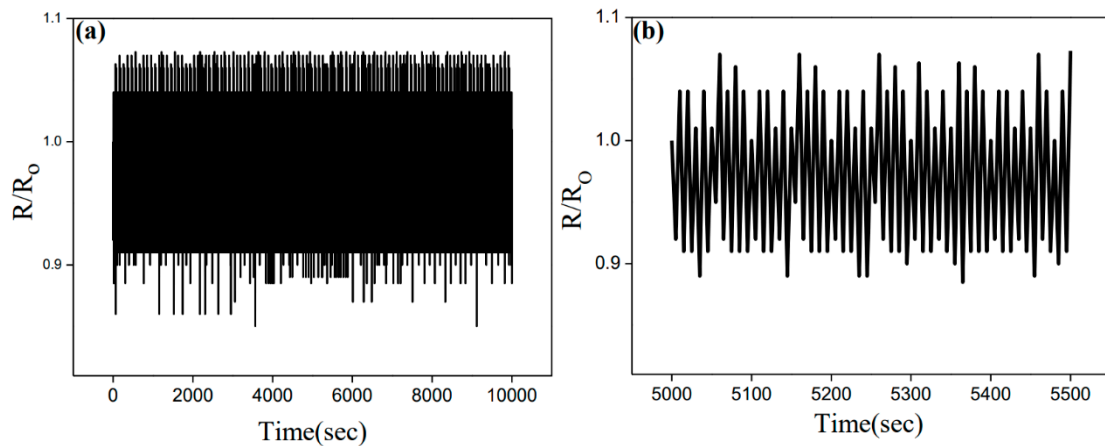


Figure S2. IG<sub>75%</sub> ionic gel: (a) change of resistance change rate under 1000 cycles and (b) amplification from 5000 s to 5500 s.

#### **References:**

1. Cellesi, F.; Tirelli, N.; Hubbell, J.A. Materials for cell encapsulation via a new tandem approach combining reverse thermal gelation and covalent crosslinking.

- Macromolecular Chemistry and Physics* **2002**, *203*, 1466-1472.
2. McCready, E.M.; Burghardt, W.R. In Situ SAXS Studies of Structural Relaxation of an Ordered Block Copolymer Melt Following Cessation of Uniaxial Extensional Flow. *Macromolecules* **2015**, *48*, 264-271.
  3. Burger, C.; Hsiao, B.S.; Chu, B. Preferred Orientation in Polymer Fiber Scattering. *Polymer Reviews* **2010**, *50*, 91-111.